Parity mix interferences and pairwise channel cancellation in the attosecond control of electron emission from H_2^+

2017 J. Phys. B: At. Mol. Opt. Phys. 50 055604

(http://iopscience.iop.org/0953-4075/50/5/055604)

IOP Publishing Journal of Physics B: Atomic, Molecular and Optical Physics
J. Phys. B: At. Mol. Opt. Phys. **50** (2017) 055604 (12pp) https://doi.org/10.1088/1361-6455/aa5255

Parity mix interferences and pairwise channel cancellation in the attosecond control of electron emission from H_2^+

D I R Boll[1] **and O A Fojón**[1,2]

[1] Instituto de Física Rosario, CONICET-UNR, Blvd. 27 de Febrero 210 bis, 2000 Rosario, Argentina
[2] Escuela de Ciencias Exactas y Naturales, FCEIA, Universidad Nacional de Rosario, Argentina

E-mail: boll@ifir-conicet.gov.ar

Received 29 July 2016, revised 10 November 2016
Accepted for publication 7 December 2016
Published 14 February 2017

Abstract

We study the single photoionization of simple diatomic molecules such as H_2^+ by a train of attopulses assisted by a near infrared laser. In particular, we focus on the so called orbital parity mix interferences leading to asymmetrical electron emission. We employ a non-perturbative model obtaining for those asymmetries analytical expressions with a functional form independent of the target structure encoding the interaction of the photoelectron with the laser field to all orders. Related to these interferences, we give conditions at which a pairwise cancellation of channels opened by the laser field occurs. Finally, we exploit the non-perturbative character of our model to analyze the dependence of the asymmetrical electron emission and the angular distribution of photoelectrons with the laser intensity. An asymmetric inhibition of the emission in the classical direction is found.

Keywords: molecules, photoionization, attopulses, laser

(Some figures may appear in colour only in the online journal)

1. Introduction

Since the emergence of attosecond science in 2001, a lot of effort was devoted to the development of tools to study and control the electron dynamics in atoms and molecules at their characteristic time and space scales [1]. The physical concept behind most of these tools is the interference of quantum-mechanical wavepackets. In turn, the possible interference mechanisms involved in the underlying atomic/molecular reactions have been studied both experimentally [2–5] and theoretically [6–12]. In particular, experiments ranging from the first characterization of attosecond pulse trains (ATPs) [2] to the more recent coherent control of molecular dynamics [3, 5] demonstrated that the interference of energy degenerate wavepackets following different quantum paths may be used to retrieve information of the system or to manipulate the reactions, respectively.

The production of ATPs commonly used in attosecond experiments is achieved through a high-order harmonic generation (HHG) process by focusing an intense ultrashort infrared laser field pulse into a noble gas atom chamber [13]. The spectrum of the resulting radiation is given by a comb of phase-locked odd harmonics of the infrared laser field that generates it. In the temporal domain, these trains have two pulses per laser period with opposite sign. On the other hand, trains generated by a laser field and its second harmonic have a spectrum given by a comb of phase-locked odd and even harmonics [14]. In this configuration, the temporal structure has only one pulse per laser period [1].

The temporal structure of ATPs may be retrieved by means of the interference between two distinct quantum paths leading to the same final state in the so called reconstruction of attosecond beating by interference of two-photon transition (RABBITT) technique [2]. Briefly, in this technique the atomic or molecular targets are exposed to the simultaneous action of an ATP and a synchronized near infrared laser (NIR) field of low intensity. The photoelectron spectrum contains principal bands mainly populated through the single-photon ionization of the target by the train of attopulses, and side-bands associated with the further absorption or emission of

one NIR photon. As a consequence of the interference between the two quantum paths that may populate the sidebands, their magnitude oscillates at twice the NIR frequency when the delay between the attopulses and the assistant laser field (henceforth delay) is modified.

More recently, the control of the orbital parity mix interference in the attosecond time scale has been experimentally demonstrated [4]. In this case, the spectrum of the ATP contains odd and even harmonics, being the relative phase shift between consecutive harmonics equal to $\pi/2$. These trains have a more complex temporal structure, not corresponding to neither of the above mentioned cases with one or two pulses per NIR cycle. The ionization of an atomic target with these ATPs in the presence of a low intensity NIR leads to an asymmetric electron emission due to parity mix interferences of energy-degenerate photoelectron distributions [4].

Due to the low NIR intensity usually employed in these experiments, the RABBITT and parity mix schemes share a common feature, i.e., the number of NIR photons absorbed or emitted by the photoelectrons in the continuum can be safely constrained to one, and thus the properties of the photoelectron spectrum are well reproduced by a second-order perturbation theory whether angle-integrated [2] or angle-resolved [4, 15] photoelectron signals are considered.

On the contrary, the intermediate NIR intensity regime, where more than one NIR photon may be exchanged, has received much less attention [16, 17]. Experimental and theoretical studies showed that the global shape of the angular distributions (ADs) in the principal bands changes significantly for different delays, as opposed to the sideband lines which are almost insensitive to the delay after normalization [18, 19].

Moreover, the presence of many interfering quantum channels in these schemes requires a theoretical treatment beyond the second-order perturbation that is not simple at all. Solving the time-dependent Schrödinger equation for reactions such as the photoionization of multi-electron atomic targets assisted by a NIR represents a challenge [20] for the current computational resources. The use of simplified models leading to predictions in reasonable agreement with *ab initio* calculations and/or experimental results reveals as a valuable option to understand the physical processes involved, as the numerical results do not often have a straightforward interpretation.

Nowadays, several models able to describe reactions assisted by a stronger NIR are available. Among them, the soft-photon approximation [21] was successfully applied to study ADs in laser-assisted atomic photoionization by photons from free electron laser [22] or HHG [18, 20] sources. Moreover, the separable Coulomb–Volkov model (SCV) revealed as a versatile alternative to provide in certain situations quite accurate results or at least in qualitative agreement with *ab initio* calculations for atomic or molecular targets [23–25].

More recently, and based on an extension of the SCV model [26], we obtained non-perturbative closed-form expressions for the AD of photoelectrons ionized by ATPs in the presence of a NIR. An excellent agreement between our analytical results and the experimental ADs for atomic targets [18, 19] was found.

In this work, we extend our previous results [26] to the case of ATPs with a non-zero phase shift between consecutive odd and even harmonics as in [4]. We analyze the ionization of molecular targets provoked by three different ATP configurations focusing on the asymmetrical electron emission. For low NIR intensities where the exchange of at most one NIR photon is expected, we show that our model resembles the usual second-order perturbation results [4]. Finally, based on the non-perturbative character of our model we study the intermediate NIR intensity range finding a partial suppression of the emission in the classical direction. This effect as well as the zeros in the ADs of photoelectrons are analyzed in term of interferences. Atomic units are used otherwise explicitly stated.

2. Theory

Let us consider the photoionization of a diatomic molecule by an ATP arising from HHG assisted by a monochromatic NIR field. We consider the case of the H_2^+ targets as its theoretical description is simpler than multielectronic molecules. Moreover, we work in the fixed nuclei approximation where the atomic centers that define the internuclear separation vector are considered to be fixed in space.

In the following, we summarize the basic ingredients of the SCV model [23–26]. As the intensity of each harmonic in the train is low due to the typical conversion efficiency in the HHG process [1], the ionization of the target may be considered to occur only through single photon processes [2]. Therefore, the interaction of the electron in the molecular ion with the train of attopulses (the fast stage of the SCV approach) may be treated in the frame of the time-dependent perturbation theory [20, 27]. On the other hand, the assistant laser field may easily induce multiphoton transitions in the continuum [2] (the slow stage of the SCV approach) thus requiring a non-perturbative treatment. Therefore, the transition matrix amplitude within the dipole approximation in the velocity gauge is given by,

$$M_{\mathrm{SCV}}(\mathbf{p}) = -\mathrm{i}\int_{-\infty}^{\infty} \mathrm{d}t\ \langle \Psi_f(\mathbf{r},t)|\mathbf{A}(t)\cdot\hat{\mathbf{p}}|\Psi_i(\mathbf{r},t)\rangle, \qquad (1)$$

where $\mathbf{p}$ is the photoelectron momentum associated to the momentum operator $\hat{\mathbf{p}}$, and $\Psi_{i,f}(\mathbf{r},t)$ are the wavefunctions in the initial and final channels of the reaction, respectively. The coordinate system used is one where $\mathbf{R}$ is the fixed internuclear separation vector pointing from nuclei 1 to 2, and $\mathbf{r}_i$ denotes the electron position vector with respect to the ith nuclei. The electron coordinate referred to the molecular center of mass will be given by $\mathbf{r} = (\mathbf{r}_1 + \mathbf{r}_2)/2$. The vector potential $\mathbf{A}(t)$ represents the APT and it can be expressed as a combination of harmonics with Gaussian envelope

$$\mathbf{A}(t) = \mathbf{\Pi}\sum_j A_j\ \mathrm{e}^{-\mathrm{i}j\omega_0 t}\mathrm{e}^{\mathrm{i}\phi_j}\mathrm{e}^{-t^2/2\tau_T^2}, \qquad (2)$$

where $\mathbf{\Pi}$ is the polarization vector, ω_0 is the fundamental frequency and ϕ_j is the individual phase of each frequency component whose amplitude is given by A_j. The full width half maximum (FWHM) duration of the train is related to the parameter τ_T through the expression $\tau_{\mathrm{FWHM}} = 2\sqrt{2\ln 2}\,\tau_T$.

As the analytical expressions for the wavefunctions in the initial and final channel of the reaction are not known some approximations must be made. First, if the NIR intensity is low ($I_L \sim 10^{11}$ W cm^{-2} in our case), and within the fixed nuclei approximation considered here, one can reasonably approximate the bound initial states by *laser-free* wavefunctions, i.e.,

$$\Psi_i(\mathbf{r}, t) = \psi_i^0(\mathbf{r})\exp(\mathrm{i}I_p t), \tag{3}$$

where I_p is the ionization potential of the initial molecular bound state given by ψ_i^0. The *laser-free* approximation is justified for the NIR intensities of interest in our work as in [28]. This is in agreement also with a large value of the Keldysh parameter γ ($\gamma \gg 10$ in our case), indicating that the NIR laser field does not induce important modifications to the Coulomb potential, i.e., the NIR may ionize the target only by a multiphoton ionization, a process which is unlikely to occur with the considered NIR intensities as compared to the single-photon ionization by the APT. The initial molecular bound state is represented by a two center development in terms of Slater type orbitals (STOs) located on each nuclei,

$$\psi_i^0(\mathbf{r}) = \sum_i c_i^{(1)}\phi_i(\mathbf{r}_1) + \sum_j c_j^{(2)}\phi_j(\mathbf{r}_2), \tag{4}$$

where $\phi_i(\mathbf{r})$ are STOs [25].

On the other hand, Ψ_f is approximated by the Coulomb–Volkov ansatz [24] in which the interaction of the ejected electron with both the residual ionic target and the laser bath is taken into account to all orders,

$$\Psi_f(\mathbf{r}, t) = \psi_f^0(\mathbf{r})\exp\left\{-\frac{\mathrm{i}}{2}\int^t [\mathbf{p} + \mathbf{A}_L(t')]^2\ \mathrm{d}t'\right\}, \tag{5}$$

with $\mathbf{A}_L(t)$ the vector potential describing the NIR field. The wavefunction $\psi_f^0(\mathbf{r})$ describes the continuum state of the molecule, and is given by,

$$\psi_f^0(\mathbf{r}) = (2\pi)^{-3/2}\mathrm{e}^{\mathrm{i}\mathbf{p}\cdot\mathbf{r}}N_p^2\ G(\mathbf{r}_1)G(\mathbf{r}_2), \tag{6}$$

where $N_p = \Gamma(1 + \mathrm{i}\nu)\ \exp(\pi\nu/2)$, $G(\mathbf{r}_i) = F_1(-\mathrm{i}\nu_i;\ 1;\ -\mathrm{i}\nu_i;\ 1;\ -\mathrm{i}(pr_i + \mathbf{p}\cdot\mathbf{r}_i))$ is the confluent hypergeometric function, $\nu_i = Z_i/p$ is the Sommerfeld parameter, where Z_i is the residual effective charge of the i-esime center.

For the sake of simplicity, we consider a linearly polarized NIR with a vector potential given by,

$$\mathbf{A}_L(t) \simeq -\frac{\mathbf{E}_1}{\omega_0}\sin(\omega_0 t - \phi_L), \tag{7}$$

and, consequently,

$$\mathbf{E}_L(t) = -\frac{\partial \mathbf{A}_L(t)}{\partial t} \simeq \mathbf{E}_1\cos(\omega_0 t - \phi_L), \tag{8}$$

where E_1 is the amplitude of the corresponding electric field and $\phi_L = \omega_0 t_0$ is an arbitrary phase that allows to modify the delay t_0.

Replacing equations (2), (3), (5) and (7) into equation (1), recognizing that in the velocity gauge time and space integrals are separable and making use of the Jacobi–Anger expansions [29], the transition amplitude given by equation (1) results,

$$M_{\mathrm{SCV}}(\mathbf{p}) = -\mathrm{i}\sqrt{2\pi}\,\tau_T M_{\mathrm{ph}}(\mathbf{p}) \sum_{m,n=-\infty}^{\infty}\sum_j \mathrm{i}^n(-1)^m A_j J_m(M)J_n(N)\mathrm{e}^{-\mathrm{i}(2m+n)\phi_L}\mathrm{e}^{\mathrm{i}\phi_j}\mathrm{e}^{-\omega_j^2\tau_T^2/2}, \tag{9}$$

where we have defined,

$$M = E_1^2/(2\omega_0)^3 = U_p/2\omega_0, \tag{10}$$

$$N = \mathbf{p}\cdot\mathbf{E}_1/\omega_0^2, \tag{11}$$

$$\omega_j = p^2/2 + I_p + (2M + 2m + n - j)\omega_0, \tag{12}$$

where $p = |\mathbf{p}|$ is the asymptotic momentum modulus and U_p is the ponderomotive energy. The monochromatic transition matrix element $M_{\mathrm{ph}}(\mathbf{p})$ is given by,

$$M_{\mathrm{ph}}(\mathbf{p}) = -\mathrm{i}\langle\psi_f^0(\mathbf{r})|\mathbf{\Pi}\cdot\nabla|\psi_i^0(\mathbf{r})\rangle. \tag{13}$$

To obtain $M_{\mathrm{ph}}(\mathbf{p})$, we employ the Coulomb continuum (CC) model [23, 24]. Further details can be found in [25].

As we showed recently [26], it is possible to give closed forms for the triple sum in equation (9) when the amplitudes A_j and phases ϕ_j are considered as constants and the asymptotic photoelectron energy satisfy the relation $p_q^2/2 + I_p + U_p = q\omega_0$, where p_q is the asymptotic photoelectron momentum associated to the q line. Briefly, if the APT is an odd-only combination of in-phase harmonics the principal bands represent the interference of energy-degenerate continuum states associated with the absorption of different harmonics from the APT and the exchange of an even number of NIR photons. In the low NIR intensity limit these lines are mainly populated by the transition involving the absorption of a given harmonic in the APT. Accordingly, they are described by an odd integer number q and their transition matrix amplitude is given by,

$$M_{\mathrm{SCV}}(\mathbf{p}_q) \propto M_{\mathrm{ph}}(\mathbf{p}_q)\mathrm{e}^{\mathrm{i}M\sin(2\phi_L)}\cos(\mathbf{p}_q\cdot\mathbf{R}_L/2),\ \ (q\ \text{odd}), \tag{14}$$

where $\mathbf{R}_L = 2\mathbf{E}_1\cos\phi_L/\omega_0^2$ [26]. Moreover, sideband lines result from the interference of energy-degenerate continuum states associated with the absorption of different harmonics from the APT and the exchange of an odd number of NIR photons. In the low NIR intensity limit they are mainly populated by transitions involving the absorption of either two consecutive odd harmonics of the APT plus the absorption and emission of one NIR photon, respectively. Accordingly, they are described by an even integer number q and their transition matrix amplitude is given by,

$$M_{\mathrm{SCV}}(\mathbf{p}_q) \propto M_{\mathrm{ph}}(\mathbf{p}_q)\mathrm{e}^{\mathrm{i}M\sin(2\phi_L)}\sin(\mathbf{p}_q\cdot\mathbf{R}_L/2).\ (q\ \text{even}). \tag{15}$$

Alternatively, if the APT is an even–odd combination of in-phase harmonics no distinction between principal bands and sidebands is possible and we obtain,

$$M_{\mathrm{SCV}}(\mathbf{p}_q) \propto M_{\mathrm{ph}}(\mathbf{p}_q)\mathrm{e}^{\mathrm{i}M\sin(2\phi_L)}\,\mathrm{e}^{\mathrm{i}\mathbf{p}_q\cdot\mathbf{R}_L/2}.\ (q\ \text{integer}). \tag{16}$$

Therefore, the transition matrix amplitudes in equations (14)–(16) may be used to calculate the differential cross section of photolines satisfying the above conditions as,

$$\frac{\mathrm{d}\sigma}{\mathrm{d}\Omega_e}(\mathbf{p}_q) \propto |M_{\mathrm{ph}}(\mathbf{p}_q)|^2 \cos^2(\mathbf{p}_q \cdot \mathbf{R}_L/2), \quad (q \text{ odd}), \tag{17}$$

$$\frac{\mathrm{d}\sigma}{\mathrm{d}\Omega_e}(\mathbf{p}_q) \propto |M_{\mathrm{ph}}(\mathbf{p}_q)|^2 \sin^2(\mathbf{p}_q \cdot \mathbf{R}_L/2), \quad (q \text{ even}), \tag{18}$$

$$\frac{\mathrm{d}\sigma}{\mathrm{d}\Omega_e}(\mathbf{p}_q) \propto |M_{\mathrm{ph}}(\mathbf{p}_q)|^2, \quad (q \text{ integer}) \tag{19}$$

respectively, where $\mathrm{d}\Omega_e = \sin\theta_e \mathrm{d}\theta_e \mathrm{d}\phi_e$ is the differential solid angle element in the photoelectron emission direction as measured from the polarization vector $\mathbf{\Pi}$.

A detailed analysis about the physical interpretation of the vector $\mathbf{R}_L$ as well as the expected behavior in the low NIR intensity limit of the above expressions can be found in [26].

3. Results and discussion

In the following, we compute spectra for the laser-assisted photoionization of fixed-in-space diatomic molecules in the parallel detection geometry (PDG $\pm$; $\theta_e = 0, \pi$) for APTs with odd or even–odd combination of in-phase harmonics in the presence of a low intensity NIR. We study H_2^+ targets as its theoretical treatment is simple and constitutes a benchmark for more complicated diatomic molecules.

Moreover, we consider the case where the APT is a combination of not-in-phase even–odd harmonics as in [4]. Finally, for this configuration the dependence of the ADs with the NIR intensity is examined.

Throughout this paper, we use the GAMESS software package [30] at the restricted open-shell Hartree–Fock level of theory to obtain the initial molecular bound state. A medium size [4s2p1d] polarized basis set of atomic STOs [31] was used by means of a STO-6G expansion [32]. Choosing the internuclear distance equal to the equilibrium value $R = 2$ leads to an ionization potential $I_p = 1.1019$. As showed in [25], monochromatic transition amplitudes calculated with the CC approximation are in qualitative agreement with numerical *ab initio* computations for the asymptotic photoelectron energies of interest.

3.1. Molecular RABBITT spectra

Atomic or molecular targets exposed to the simultaneous action of an APT (pump) and a weak NIR (probe) constitute the RABBITT scheme. The characteristic number of NIR photons exchanged by the photoelectron and the assistant laser field may be estimated from the parameter N in equation (11) as the effective number of exchanged photons N_{eff} is given by $N_{\mathrm{eff}} \sim pE_1/\omega_0^2$ [33]. To characterize the laser intensity, we refer in this work to a weak laser field when the condition $N_{\mathrm{eff}} \lesssim 1$ is fulfilled. As it will be shown later, this condition implies that the general features of the photoelectron spectrum may be obtained from a second-order perturbation theory.

When an APT prepared as a combination of in-phase odd harmonics is considered, the photoelectron spectra contains principal bands corresponding to the absorption of one photon from the APT with frequency $q\omega_0$, being q an odd integer number and thus the energy spacing between principal bands is $2\omega_0$. On the other hand, the sidebands located between principal bands are populated by two-photon processes, namely, the absorption of a photon from the APT with energy $q\omega_0$ ($q\omega_0 + 2\omega_0$) plus the absorption (emission) of a NIR photon with energy ω_0.

The sideband signal as a function of the delay oscillates at twice the NIR frequency [2] due to interferences between the two different quantum paths leading to the same energy state. On the contrary, the principal bands remain almost constant because they are mainly populated by just one quantum path. These properties may be deduced by means of a second-order perturbation theory as shown in the appendix.

On the other hand, for APTs with an even–odd combination of in-phase harmonics there is no distinction between principal bands and sidebands. Every band in the spectrum have contributions from one- and two-photon transitions. Oscillations in the signal of these bands, if any, are expected to be small due to the dominance of the one-photon transitions in the low NIR intensity case.

In figure 1, we present the photoelectron spectra in the PDG+ scheme corresponding to the photoionization of the H_2^+ molecular ion by APTs composed of the usual odd (first row) or even–odd (second row) combination of in-phase harmonics in the presence of an 800 nm probe laser with an intensity of $I_L = 1.8 \times 10^{10}$ W cm^{-2}. The APTs and the NIR are linearly polarized in the direction of the internuclear separation vector $\mathbf{R}$.

The expected behavior is obtained for the spectrum in figure 1(a) where a second-order perturbative expansion of equation (9) is considered (see appendix). The principal bands as a function of the delay are constant whereas the sidebands oscillate at twice the NIR frequency. If the exchange of a larger number of NIR photons is allowed (panel (b)), the appearing of small oscillations in the odd harmonics bands as well as a decrease in the sidebands intensity is observed. However, as the assistant laser field is weak ($N_{\mathrm{eff}} \simeq 0.78 \sim 1$) no major discrepancies are expected and the spectra remain essentially the same as can be seen comparing panels (a) and (b).

On the contrary, when the APT is a combination of in-phase even–odd harmonics (figure 1(c)), every band in the spectrum present small oscillations as a function of the delay. When the exchange of a larger number of photons is allowed, the small oscillations seen in the one NIR photon case are almost erased as can be observed in panels (c) and (d) of figure 1. This result is in agreement with our theoretical finding given by equation (19), where a differential cross section independent of the delay is obtained for these APTs when the intensity of the harmonics is constant.

So far, the two cases analyzed have common features. First, as the NIR intensity is low, the probability for the exchange of more than one photon between the photoelectron in the continuum and the assistant laser field is small and, thus, a second-order perturbation treatment is usually enough

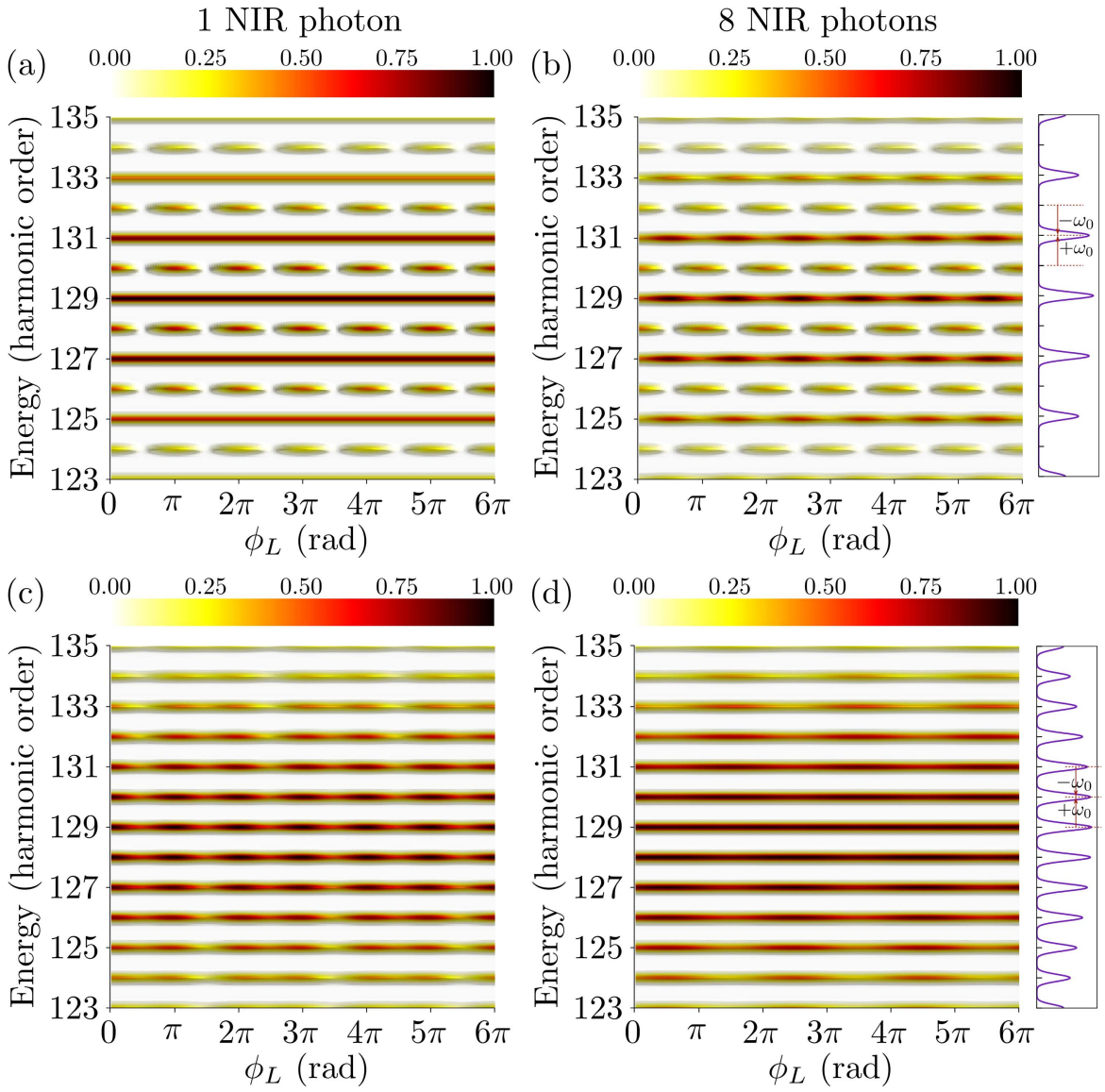

Figure 1. (a) Photoelectron spectrum as a function of the delay admitting the exchange of at most one NIR photon, in the PDG+, for H_2^+ at $R = 2$. The APT and the NIR are linearly polarized along **R**. The APT contains only odd in-phase harmonics with $\tau_T = 150$. The NIR wavelength and intensity are 800 nm and $I_L = 1.8 \times 10^{10}$ W cm^{-2}, respectively. (b) Same as (a) but allowing the exchange of at most 8 NIR photons. (c) Same as (a) but with an APT composed of even–odd harmonics. (d) Same as (c) but allowing the exchange of at most 8 NIR photons.

to describe the main characteristics of the spectra. Also, the electron emission in the PDG ± directions is symmetric regardless of the delay. As will be shown in the next section, this up–down symmetry is broken for APTs with an even–odd combination of not-in-phase harmonics.

3.2. Orbital parity mix

Let us consider an APT with a relative phase difference between consecutive even and odd harmonics of $\pi/2$ and a weak NIR, colinearly polarized along the internuclear separation vector. For atomic targets, this configuration produces asymmetrical photoelectron emission patterns due to orbital parity mix interferences [4], being the corresponding phases ϕ_j responsible for those asymmetries.

In figure 2, we show the photoelectron spectra as function of the delay and the asymptotic photoelectron energy expressed in terms of the harmonic order q. In coincidence with the RABBITT scheme studied before, the exchange of a larger number of NIR photons (panels (b) and (d)) does not induce any remarkable change in the spectra as compared with the case in panels (a) and (c) where at most one NIR photon is exchanged.

On the other hand, an up–down asymmetry is observed for these APTs. A comparison between panels in the first and second row of figure 2 reveals that the oscillations as a function of the delay in the PDG ± directions are out of phase. Besides, these oscillations now have a frequency equal to the NIR one.

For a low NIR intensity, this asymmetry may be deduced from the second-order perturbative limit of our model, where

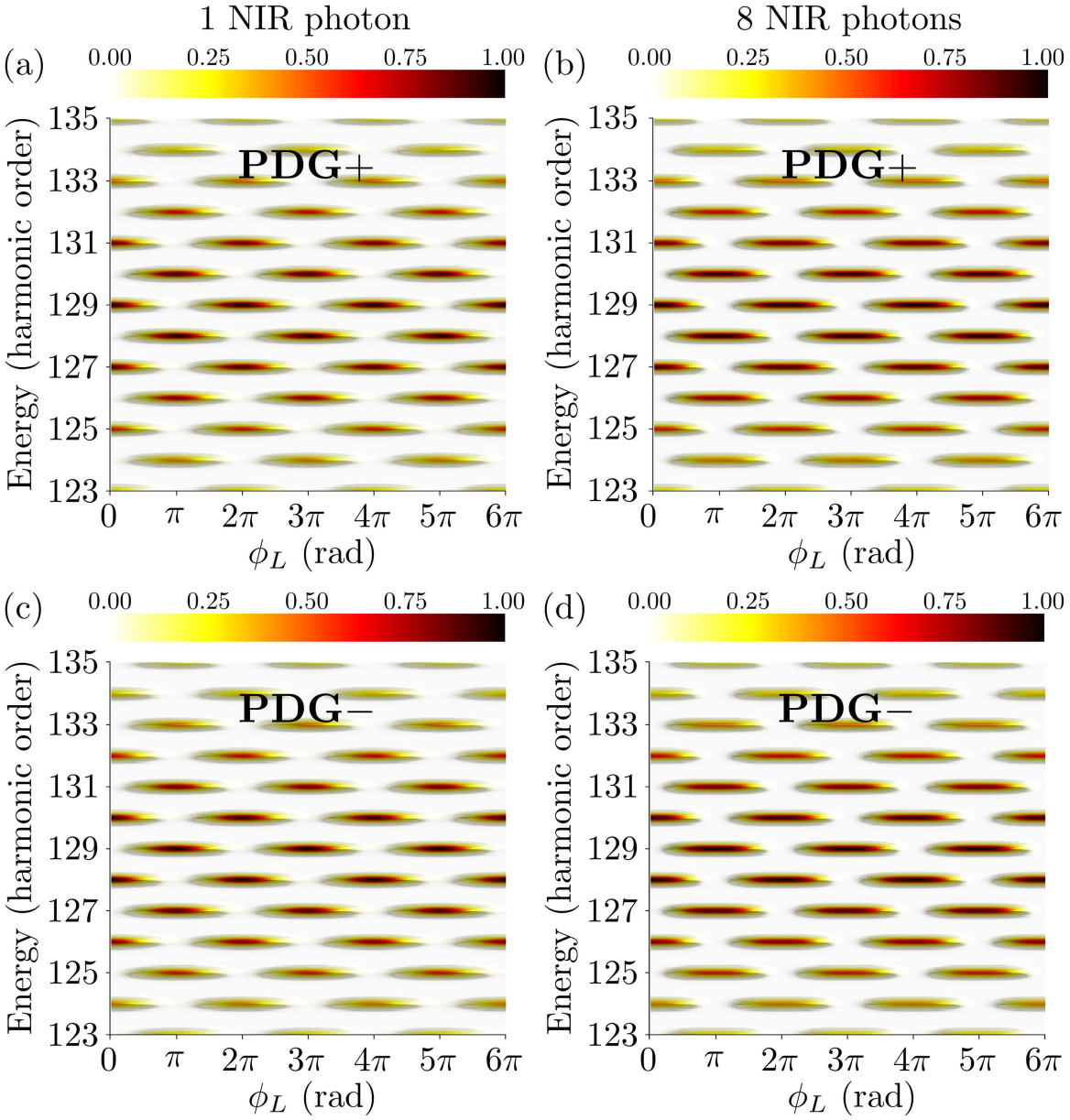

Figure 2. (a) Photoelectron spectrum as a function of the delay, in the PDG+ scheme, for H_2^+ at $R = 2$. The APT contains even–odd harmonics with $\phi_j = +\pi/4\,(-\pi/4)$ if j is odd (even). The APT and the NIR are linearly polarized along **R**. The remaining parameters are the same as in figure 1. (b) Same as (a) but allowing the exchange of at most 8 NIR photons. (c) Same as (a) but in the PDG − scheme. (d) Same as (c) but allowing the exchange of at most 8 NIR photons.

the square modulus of the transition matrix amplitude reads (see appendix),

$$\begin{aligned}|M_{\mathrm{SCV}}(\mathbf{p}_q)|^2 &\propto |J_0(N)A_q e^{i\phi_q} + i\,J_1(N)A_{q+1}e^{-i\phi_L}e^{i\phi_{q+1}} \\ &+ i^{-1}J_{-1}(N)A_{q-1}e^{i\phi_L}e^{i\phi_{q-1}}|^2 \\ &\propto J_0^2(N)A_q^2 + J_1^2(N)A_{q+1}^2 + J_1^2(N)A_{q-1}^2 \\ &+ 2J_1^2(N)A_{q-1}A_{q+1}\cos(2\phi_L + \phi_{q-1} - \phi_{q+1}) \\ &+ 2J_0(N)J_1(N)A_q[A_{q+1}\sin(\phi_L + \phi_q - \phi_{q+1}) \\ &- A_{q-1}\sin(\phi_L + \phi_{q-1} - \phi_q)],\end{aligned} \tag{20}$$

where three terms may be recognized as in [4]. The first one (DC) represents the individual contribution of one- and two-photon processes and it is independent of the delay. The second one represents the interference between two-photon processes and oscillates at twice the NIR frequency as the sidebands in the usual RABBITT scheme. The last one (FSI) encodes the interference between one- and two-photon transitions and oscillates at the NIR frequency when the delay is modified.

The expression in equation (20) is valid for all the APTs considered so far. However, trains with a combination of in-phase harmonics do not show a FSI contribution just because the intrinsic phases and the amplitudes satisfy the relations $\phi_q \sim \phi_{q\pm1}$ and $A_{q-1} \sim A_{q+1}$, thus the FSI contribution is zero. On the other hand, for APTs with a relative phase difference of $\pi/2$ between consecutive even and odd harmonics,

the particular values of ϕ_j make the FSI contribution in equation (20) different from zero. Moreover, as this is the only term with odd parity under the inversion $\mathbf{p} \to -\mathbf{p}$ through the factor $J_1(N)$, it must be responsible for the asymmetry. In addition, as this contribution represents interference between one- and two- photon transitions, the interfering wavepackets are of different parity according to the dipole selection rules.

Briefly, if the electron in the initial molecular σ state is promoted to the continuum by the absorption of one photon from the APT, its state changes to a π symmetry one in order to satisfy the dipole selection rules. The further absorption (emission) of a NIR photon by the photoelectron, changes its state to a σ and/or δ symmetry state. So, a given photoline may be populated by wavepackets having different parity, which interfere constructively on one direction and destructively in the opposite one, generating asymmetric ADs.

These asymmetries in the photoelectron spectrum are reminiscent to those in the ionization of a coherent superposition of initial electronic states [6, 34–36]. However, the underlying mechanisms responsible for the asymmetric electron emission are different. In the ionization of a coherent superposition of initial electronic states, a strong laser field acting as the pump stage of the reaction induces a resonant excitation of the target (possibly through multiphoton processes) creating thus an asymmetric initial state that generates asymmetrical electron emission when it is probed by the XUV radiation. On the contrary, in our case the assistant laser field is not able to induce significant asymmetries in the initial state due to its low intensity. However, the properties of the APT are such that interferences of energy degenerate continuum wavepackets of different parity are produced.

Alternatively, a closed-form transition matrix element for this reaction may be obtained if the amplitude of harmonics in equation (2) is considered as constant. Proceeding along the same lines as in [26], and taking into account that $\phi_j = +\pi/4$ $(-\pi/4)$ if j is odd (even), we obtain for this case

$$M_{\mathrm{SCV}} \propto M_{\mathrm{ph}}(\mathbf{p}_q)\sin(\mathbf{p}_q \cdot \mathbf{R}_L/2 \pm \pi/4), \tag{21}$$

where the $+(-)$ sign corresponds to lines with q odd (even). For these APTs, every line in the spectrum behaves as an interference of principal lines and sideband lines in the usual RABBITT scheme (APTs with odd harmonics only), as can be seen through an expansion of equation (21) with usual trigonometric identities, and thus leading to a parity mixing. The extent of this mixing can be controlled just by changing the delay ϕ_L.

Interestingly, our analytical result in equation (21) describes this parity mixing to all orders in the exchange of NIR photons, thus avoiding the cumbersome perturbative expansions needed when a stronger NIR is considered.

In figure 3, we present the three-dimensional ADs corresponding to an asymptotic photoelectron energy with $q = 129$ and different delays for the laser assisted photoionization of the H_2^+ molecular ion, with an APT and a NIR having the same properties as before (figure 2). Also, we present a monochromatic AD for the same energy. As can be seen, an up–down asymmetry is obtained for the delays

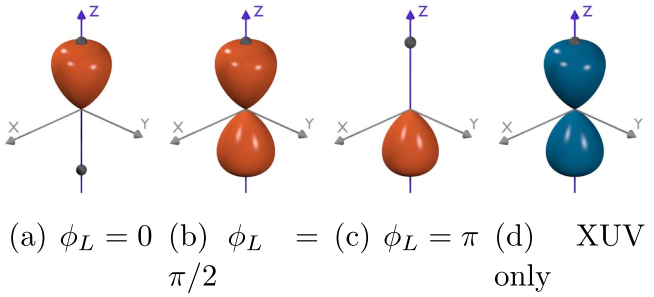

Figure 3. (a)–(c) Three-dimensional angular distributions for H_2^+ at $R = 2$, $q = 129$ and different delays. The APT and the NIR are the same as in figure 2. (d) Monochromatic angular distribution with the same asymptotic photoelectron energy.

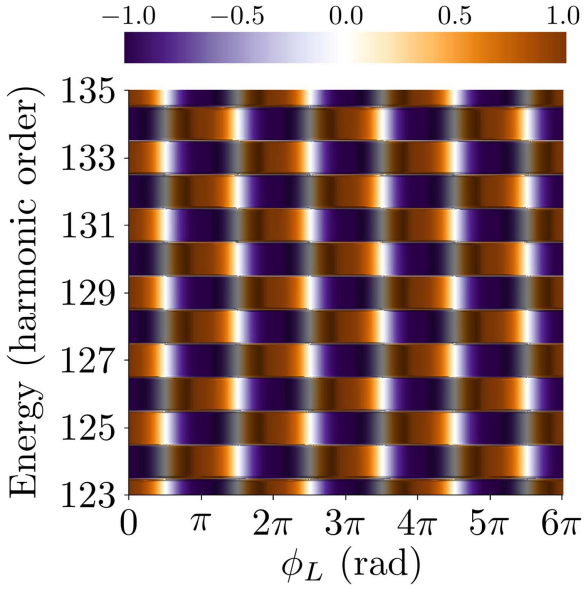

Figure 4. Asymmetry parameter A of equation (22) as a function of the delay and the photoelectron energy, calculated with the spectra in figures 2(b) and (d).

$\phi_L = 0$ and $\phi_L = \pi$. On the other hand, the AD is symmetric for $\phi_L = \pi/2$ as in the monochromatic case (panel (d)). The symmetric emission for the $\phi_L = \pi/2$ case is clearly understood by means of the equation (21), where the replacement of the ϕ_L value leads to $\mathbf{R}_L = 0$ and therefore to a matrix element where the AD depends only on the monochromatic transition amplitude $M_{\mathrm{ph}}(\mathbf{p}_q)$.

As a measure of the up–down asymmetry we adopt the parameter A, given by

$$A = \frac{|M^+_{\mathrm{SCV}}|^2 - |M^-_{\mathrm{SCV}}|^2}{|M^+_{\mathrm{SCV}}|^2 + |M^-_{\mathrm{SCV}}|^2}, \tag{22}$$

where the superscript $\pm$ indicates a photoelectron emission in the PDG $\pm$ direction.

In figure 4, we show the variation of this ratio as a function of the delay and the photoelectron asymptotic energy, calculated with the spectra in figures 2(b) and (d). As can be seen, for a fixed photoelectron energy, A oscillates between positive and negative values indicating that the preferred emission direction can be modified by adjusting the delay. On the other hand, A considered as a function of the

photoelectron energy at a fixed delay, shows a sign change in passing from a band to the next.

We remark the similarity of our calculation for the asymmetry parameter A in figure 4 and the corresponding magnitudes measured for atoms (figures 3(b) and (d) in [4]), where a checkerboard pattern was found for the odd indexed coefficients β_i in the expansion into Legendre polynomials of the measured full angular-resolved photoelectron distributions. Taking into account that our asymmetry factor A shows the total up–down asymmetry, it is proportional to the sum of all the odd-indexed expansion coefficients β_i in [4], as can be easily shown using the parity properties of the Legendre polynomials.

Interestingly, the asymmetry parameter A can be obtained in a closed form by using the analytical transition amplitudes given by equation (21), and the fact that $|M_{\rm ph}(\mathbf{p}_q)|^2 = |M_{\rm ph}(-\mathbf{p}_q)|^2$, i.e.,

$$A = \frac{\sin^2(p_q R_L/2 \pm \pi/4) - \sin^2(-p_q R_L/2 \pm \pi/4)}{\sin^2(p_q R_L/2 \pm \pi/4) + \sin^2(-p_q R_L/2 \pm \pi/4)}, \quad (23)$$

where the $+(-)$ corresponds to lines with q odd (even). Expanding the trigonometric functions we obtain,

$$A = \pm\sin(p_q R_L). \quad (24)$$

This expression, whose functional form is independent of the target structure, contains the interaction between the photoelectron and the NIR to all orders. Moreover, it indicates that the change in sign observed when passing from odd harmonic lines to even ones (and vice versa) may be attributed to the particular temporal structure of the APT. On the other hand, the oscillation observed for a fixed photoelectron energy depends on the laser intensity and the delay ϕ_L. Moreover, taking into account that the NIR intensity is low, an expansion of the sine factor in equation (24) in Bessel functions retaining only the first term leads to the following dependence with the delay,

$$A \propto \pm J_1\left(\frac{2p_q E_1}{\omega_0^2}\right)\cos\phi_L, \quad (25)$$

that qualitatively explains the observed oscillation at a fixed photoelectron energy. Under these conditions, fitting A with the first two terms of the expansion in Bessel functions yields a nearly perfect match with the results obtained with the full expression of equation (9).

As will be shown in next section, equation (24) predicts more complex oscillations for A at higher NIR intensities, leading to a sub-femtosecond control of the asymmetric electron emission as a function of the delay.

3.3. Dependence with the NIR intensity

For higher NIR intensities, the second-order perturbation expansion in equation (20) is no longer appropriate to describe the photoelectron spectrum because the number of NIR photons exchanged by the photoelectron and the laser bath may be larger than one. Instead, the transition matrix amplitude must be calculated with the full expression in equation (9) or the analytical result in equation (21).

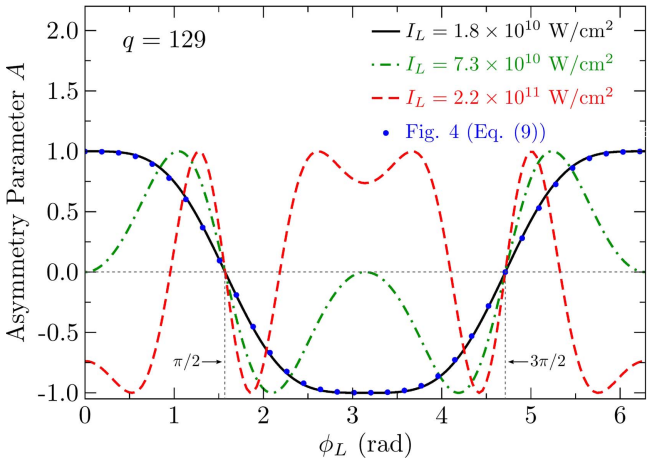

Figure 5. Asymmetry factor A computed with equation (24) as a function of the delay for a photoline with $q = 129$ and different NIR intensities. The blue bullet values are extracted from figure 4.

In order to study the dependence of the up–down asymmetry with the laser intensity we calculate A by means of equation (24) for different NIR intensities and a photoelectron energy corresponding to the spectral line with $q = 129$. These asymmetry parameters are shown in figure 5.

The lowest NIR intensity considered coincides with the value used in figure 4, therefore we compare the results of the latter with those obtained with equation (24). As can be seen, a nearly perfect match is obtained, despite that the results in figure 4 are calculated with non-constant harmonic amplitudes A_j. Additionally, it can be seen that the asymmetry parameter A deviates from the pure cosine dependence with the delay obtained in equation (25). This behavior may be related to contributions associated with the exchange of three NIR photons, as observed previously for atomic targets (figure 3(d) in [4]). However, in the latter the influence of these contributions is smaller due to a weaker coupling between the photoelectron and the laser field, inferred from the characteristic number $N_{\rm eff} \sim 0.43$ [4] which is roughly half of the value in our simulations.

Moreover, to achieve a total inversion of the electron emission direction for low NIR intensities it is necessary to change the ϕ_L value from 0 to π (or, alternatively, from π to 2π). In turn, this change is connected to a variation of the delay between the APT and the assistant laser field of π/ω_0 that ammounts to half of the laser period ($T_L = 2\pi/\omega_o \sim 2.7$ fs). On the contrary, for higher NIR intensities it is possible to obtain an inversion of the photoelectron emission direction by smaller changes of the delay as can be seen in the dashed curve in figure 5. The higher the NIR intensity, the shorter the delay shift necessary to invert this emission direction. This shortening of the delay change implies that higher-order continuum–continuum transitions are involved, i.e., the photoelectron is able to exchange more than one photon with the assistant laser field.

In addition, for delays that satisfy the relation $\phi_L = (2k+1)\pi/2$, the electron emission is symmetric independently of the NIR intensity, as can be seen in figure 5

where $A = 0$ for $\phi_L = \pi/2, 3\pi/2$. This feature, which can be related to the fixed position of the minima in the sideband signal for usual RABBITT experiments [37], may be explained in terms of what we call pairwise channel cancellation (PCC) analysis. By means of this PCC analysis, we are able to establish the conditions under which the contributions corresponding to the absorption and emission of n NIR photons cancel each other pairwise. The PCC condition is given by the simple relation (see appendix),

$$\cos(n\phi_L) = 0. \tag{26}$$

Applying the PCC condition to the case $\phi_L = (2k + 1)\pi/2$, we conclude that in this case the exchange of an odd number of NIR photons cancel each other pairwise regardless of the NIR intensity. Moreover, as the asymmetrical electron emission in the parity mixing requires that the channels involving the exchange of an even and odd number of NIR photons are open, and the latter ones cancel due to the PCC, parity mix interferences leading to asymmetrical electron emission are not possible. Therefore, the photoelectron ADs for these delay values (a half-integer multiple of π) are necessarily symmetric.

On the contrary, for delays other than $\phi_L = (2k + 1)\pi/2$ it is possible to induce an inversion of the most favored emission direction by changing the NIR intensity, as can be seen comparing the results for the highest and lowest NIR intensities in figure 5.

To study the dependence of the ADs with the laser intensity, we have computed the angle-energy photoelectron spectra for two different delays and NIR intensities. These spectra are shown in figure 6. As expected, the increase of the NIR intensity has different consequences on the spectrum according to the delay. For $\phi_L = \pi/2$, the spectra do not evidence major differences, remaining essentially the same for both intensities, even if higher order continuum–continuum transitions are involved in the higher intensity case. Qualitatively, this may be explained as before taking into account that the PCC analysis implies that only transitions with exchange of an even number of NIR photons are effectively allowed and they cannot modify strongly the ADs as they posses the same symmetry. Quantitatively, equation (21) indicates that the transition matrix amplitude for this delay is independent of the NIR intensity (as $\mathbf{R}_L = 0$) and therefore no major changes should be expected.

On the other hand, large differences can be seen between the spectra for $\phi_L = \pi/4$ at different intensities. First, the most favored electron emission direction is reversed, i.e., for every band in the spectrum, electrons emitted upwards (downwards) in the low NIR intensity case are ejected mainly in the opposite direction when the intensity is increased. This fact could allow to control the main electron emission direction just by tuning the NIR intensity.

Moreover, for the higher intensity a partial suppression of the emission is observed at the ejection angles $\theta_e = 0$ or π. The origin of these dips in the classical emission direction can be traced to the evolution of angle-resolved photoemission spectra in the multi-color ionization of atomic targets, where a critical dependence with the delay and the relative harmonic phases was found [17, 18, 26].

To study the interference effects involved in this emission pattern, in figure 7 we show the two-dimensional ADs corresponding to the photoline with $q = 129$, $\phi_L = \pi/4$ and the higher NIR intensity. The AD obtained with the full expression of equation (9) (full line) shows an asymmetric electron emission and also the existence of angles at which the emission is forbidden. In this case, a PCC analysis (only) predicts the absence of contributions from channels with $|n| = 2, 6$, etc.

The dip at the ejection angle $\theta_e = 0$ is a consequence of interferences between channels opened by the NIR as observed for sideband lines at intermediate NIR intensities [26], enhanced by the asymmetric emission induced by the temporal structure of the APT. These properties are encoded in the interference factor of equation (21).

On the other hand, the physical origin of the zeros in the ADs may be understood if the monochromatic transition amplitude in equation (21) is approximated by a plane wave model (PW) [38, 39]. In the PW model, the monochromatic transition amplitude is proportional to $\cos\theta_e \cos(\mathbf{p}\cdot\mathbf{R}/2)$. The corresponding AD calculated with equation (21) is shown in figure 7 by a dashed–dotted line. In this way, the zero labeled as A at $\theta_e = \pi/2$, comes from the $\cos\theta_e$ factor, i.e., the transition amplitude from an atomic center initially in a 1s orbital is zero for an emission direction perpendicular to the APT polarization. Moreover, the zeros B and C symmetrically placed around $\pi/2$ arise from the total destructive interferences due to coherent emission from both molecular centers. Their angular position is dictated by the interference factor $\cos(\mathbf{p}\cdot\mathbf{R}/2)$ and thus they strongly depend on the target structure through the internuclear separation vector $\mathbf{R}$.

Additionally, there is another zero (D) whose origin is the total destructive interference of channels opened by the NIR. This zero is placed close to C, and its angular position is given by the condition $\sin(\mathbf{p}_q\cdot\mathbf{R}_L/2 + \pi/4) = 0$. This expression, extracted from the interference term in equation (21), indicates that its angular position depends on the NIR intensity, the delay and the asymptotic photoelectron momentum.

The influence of the Coulomb interaction between the ejected photoelectron and the remaining ion is evidenced when the full calculation is compared to the one using the PW approximation. Even for this photoelectron energy, differences of about 20% are observed at the emission angle $\theta_e = \pi$. Moreover, due to the Coulomb interaction the position of the nodes in the ADs are shifted to values slightly closer to $\pi/2$, as compared to the PW case. In turn, this shift causes the collapse of the zeros C and D into a single node when the Coulomb interaction is taken into account.

Besides, in figure 7 the dashed line corresponds to the AD of a fictitious atomic target initially in a 1s orbital, with the same ionization potential as the molecule. Its AD differs from the PW model for the molecular case in the interference factor $\cos(\mathbf{p}\cdot\mathbf{R}/2)$.

Finally, the AD for the atomic target and the molecular one in the PW approximation are unexpectedly similar for

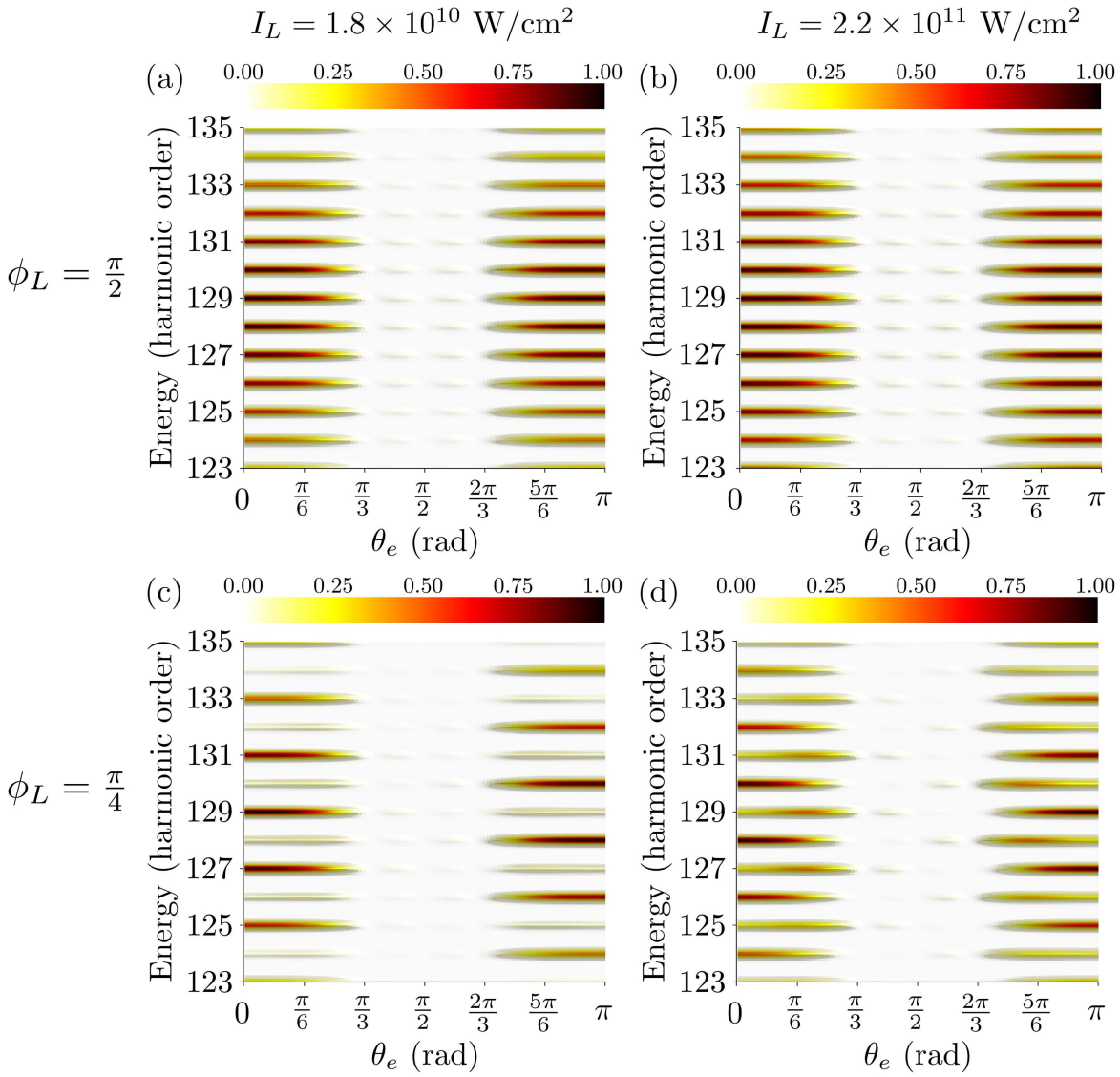

Figure 6. Angle-energy spectra as a function of the photoelectron ejection angle θ_e and energy, calculated for different NIR intensities I_L and delays ϕ_L.

emission angles between $\pi/2$ and π. This behavior is a consequence of the proximity of zeros C and D. On the contrary, for emission angles near the B zero, they are clearly different due to the absence of interferences from the coherent emission of both molecular centers in the atomic case.

4. Conclusions

We have extended our previous *non-perturbative* model [26] to take into account the case of APTs with non-zero relative phase between consecutive even–odd harmonics.

We have focused for simplicity on the case of H_2^+ but our general conclusions remain valid for more complex diatomic molecular targets. In the low NIR intensity regime, we have shown that our model admits an expansion that yields results similar to those of a second-order perturbative theory.

Moreover, employing our model we are able to reproduce qualitatively the spectra expected for the RABBITT pump-probe photoionization reaction of fixed-in-space molecules. We also show that APTs with intrinsic phases of $+\pi/4$ (odd harmonics) and $-\pi/4$ (even harmonics) lead to asymmetric emission patterns due to orbital parity mixing as in the atomic case [4]. Even if our results are obtained for the specific values of the phases listed above, it is a simple matter to show that they are also valid for APTs with a $\pi/2$ phase shift between consecutive odd and even harmonics.

We have studied the up–down asymmetries in the ejected electron ADs by defining an adequate asymmetry parameter. Even if we are dealing with molecular targets, our findings resemble the ones observed in the case of atoms where a checkerboard pattern was found under definite conditions [4]. As a matter of fact, considering APTs with constant harmonic amplitudes we find an analytical expression for the up–down asymmetry with a functional form independent of the target structure. In addition, this expression contains the interaction of the photoelectron and the laser bath to all orders. In particular, this analytical result shows that it would be possible to

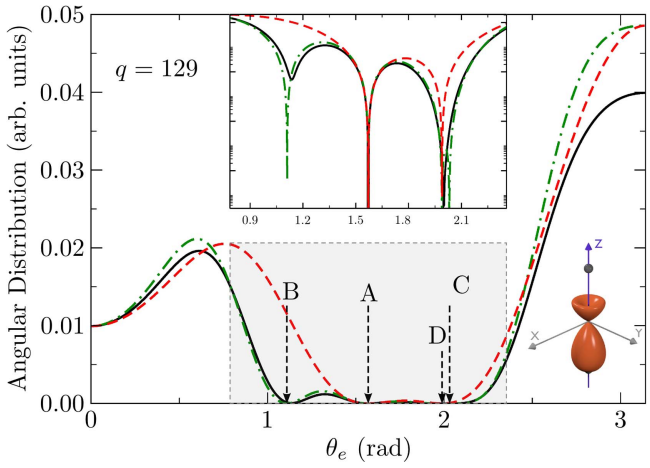

Figure 7. Two-dimensional angular distributions for H_2^+ at $R = 2$ normalized at $\theta_e = 0$, with an APT as in figure 2 and a collinear NIR of intensity 2.2×10^{11} W cm^{-2}. The full-line results are obtained with equation (9) and monochromatic transition elements from the CC model. The dashed–dotted line results are obtained with equation (21) and monochromatic transition elements from the PW model. The dashed line results, corresponding to a fictitious atom, are obtained with equation (21) (see text for details). The upper-center inset shows the gray-shaded area in logarithmic scale. The right-bottom inset shows three-dimensional angular distribution calculated from equation (9).

control the photoelectron emission direction through sub-femtosecond variations of the delay just by increasing the NIR intensity.

In addition, we find the condition to be satisfied for what we call PCC that reveals as an extremely useful tool to elucidate and attribute the physical origin of some particular symmetrical electron emissions to the absence of orbital parity mix interferences. Besides, we verify a partial suppression for the emission in the classical direction in the molecular case. The associated dips in the electron ADs may be interpreted as coming from interferences between channels opened by the NIR presence.

Finally, we discuss the physical origin of the zeros appearing in the AD based on the different mechanisms of interferences. A comparison with atomic results and the influence of the Coulomb interaction are also considered.

Acknowledgments

Authors acknowledge financial support from the Agencia Nacional de Promoción Científica y Tecnológica (PICT No. 01912), the Consejo Nacional de Investigaciones Científicas y Técnicas de la República Argentina (PIP No. 11220090101026), and the Fundación Josefina Prats.

Appendix

We summarize the approximations performed to obtain a perturbative second-order expansion of the observables in the laser-assisted photoionization process as well as the PCC condition.

The sum in m in equation (9) may be replaced by the term with $m = 0$, $J_0(M) \sim 1$, provided that $M \ll 1$. Besides, for APTs with several pulses we have that $\tau_L \gg 1$, and thus the Gaussian factor in equation (9) gives a non-negligible contribution only when $\omega_j \sim 0$, i.e.,

$$\frac{p^2}{2} + I_p + U_p + (n - j)\omega_0 \sim 0. \tag{A.1}$$

If $\mathbf{p}_q$ corresponds to the momentum of a photoelectron in the q-esime band of the spectrum, then the following relation must be verified,

$$\frac{p_q^2}{2} + I_p + U_p - q\omega_0 \sim 0 \tag{A.2}$$

and replacing it in equation (A.1) we obtain,

$$j = n + q. \tag{A.3}$$

Using this relation we can finally write the transition matrix element as,

$$M_{\mathrm{SCV}}(\mathbf{p}_q) \propto \sum_n \mathrm{i}^n A_{n+q} J_n(N) \mathrm{e}^{-\mathrm{i}n\phi_L} \mathrm{e}^{\mathrm{i}\phi_{n+q}}. \tag{A.4}$$

Now, expanding the square modulus of the preceding equation, and keeping contributions up to the first order, we obtain,

$$\begin{aligned} |M_{\mathrm{SCV}}(\mathbf{p}_q)|^2 &\propto |J_0(N) A_q \mathrm{e}^{\mathrm{i}\phi_q} + \mathrm{i}\, J_1(N) A_{q+1} \mathrm{e}^{-\mathrm{i}\phi_L} \mathrm{e}^{\mathrm{i}\phi_{q+1}} \\ &\quad + \mathrm{i}^{-1} J_{-1}(N) A_{q-1} \mathrm{e}^{\mathrm{i}\phi_L} \mathrm{e}^{\mathrm{i}\phi_{q-1}}|^2 \\ &\propto J_0^2(N) A_q^2 + J_1^2(N) A_{q+1}^2 + J_1^2(N) A_{q-1}^2 \\ &\quad + 2J_1^2(N) A_{q-1} A_{q+1} \cos(2\phi_L + \phi_{q-1} - \phi_{q+1}) \\ &\quad + 2J_0(N) J_1(N) A_q [A_{q+1} \sin(\phi_L + \phi_q - \phi_{q+1}) \\ &\quad - A_{q-1} \sin(\phi_L + \phi_{q-1} - \phi_q)]. \end{aligned} \tag{A.5}$$

Three terms are recognized, namely, DC, RABBITT and FSI as in the second-order perturbation theory [4], from which the labels are taken.

In the following, we study the contributions coming from the DC, RABBITT and FSI terms for different ATPs designs. In addition, we give the condition for the occurrence of the PCC.

ATPs with odd harmonics, $\phi_j = 0$

In this case, the APT spectrum is composed of odd harmonics solely. However, the presence of a NIR populates the even harmonics energy region between consecutive odd harmonics by two-photon processes. We consider these two cases separately.

If q is odd, then $q \pm 1$ is even, so $A_{q\pm1} = 0$ and $A_q \neq 0$. Only the DC contribution associated to $J_0(N)$ survives and so there is no dependence with the delay (see figure 1(a)).

If q is even, then $q \pm 1$ is odd, so $A_{q\pm1} \neq 0$ and $A_q = 0$. As expected [2], the sidebands present DC contributions associated to the $J_1(N)$ functions and the RABBITT

contributions, oscillating thus at twice the NIR frequency when considered as a function of the delay (see figure 1(a)).

ATPs with odd and even harmonics, $\phi_j = 0$

In this case, there is no need to consider the even and odd cases separately. As $A_q \neq 0$ for all q, both the DC and the RABBITT contributions are present in all bands. However, if $J_0(N) \gg J_1(N)$ the oscillating RABBITT contribution is expected to be small (see figure 1(c)). Moreover, the FSI contribution cancels due to the properties $A_{q-1} \sim A_{q+1}$ and $\phi_j = 0$. Therefore, no up–down asymmetries are expected.

Odd and even harmonics, $\phi_j = \pm\pi/4$

Again, as $A_q \neq 0$ for all q, both DC and RABBITT contributions are present in all bands. Also, the sign inversion in the differences $\phi_q - \phi_{q-1} = \pm\pi/2$ and $\phi_{q+1} - \phi_q = \mp\pi/2$ for q fixed with $A_{q-1} \sim A_{q+1}$ allows to write the terms inside square brackets in equation (A.5) as a sum of $\cos\phi_L$ terms, giving a non-zero FSI contribution.

Pairwise channel cancellation

We look for the conditions under which the contributions corresponding to the absorption and emission of n NIR photons cancel each other. If the amplitudes A_{n+q} in equation (A.4) are all equal and constant, and recalling that $J_{-n} = (-1)^n J_n$, the condition for the mutual cancellation of the terms corresponding to n and $-n$ in equation (A.4) is,

$$e^{-in\phi_L} e^{i\phi_{n+q}} = -e^{in\phi_L} e^{i\phi_{-n+q}}. \tag{A.6}$$

Now, defining the phase difference $\Delta = \phi_{-n+q} - \phi_{n+q}$, this condition reads,

$$\cos(n\phi_L + \Delta/2) = 0. \tag{A.7}$$

When this relation is verified, we talk of PCC.

Finally, taking into account that $\Delta = 0$ in all the cases considered in this work, we obtain the result given by equation (26).

References

[1] Vrakking M J J 2014 *Phys. Chem. Chem. Phys.* **16** 2775–89
[2] Paul P M, Toma E S, Breger P, Mullot G, Aug F, Balcou P, Muller H G and Agostini P 2001 *Science* **292** 1689–92
[3] Kelkensberg F *et al* 2011 *Phys. Rev. Lett.* **107** 043002
[4] Laurent G, Cao W, Li H, Wang Z, Ben-Itzhak I and Cocke C L 2012 *Phys. Rev. Lett.* **109** 083001
[5] Ranitovic P *et al* 2014 *Proc. Natl Acad. Sci.* **111** 912–7
[6] Yudin G L, Bandrauk A D and Corkum P B 2006 *Phys. Rev. Lett.* **96** 063002
[7] He F, Ruiz C and Becker A 2007 *Phys. Rev. Lett.* **99** 083002
[8] He F, Ruiz C and Becker A 2008 *J. Phys. B: At. Mol. Opt. Phys.* **41** 081003
[9] Fernández J and Martín F 2009 *New J. Phys.* **11** 043020
[10] Picón A, Bahabad A, Kapteyn H C, Murnane M M and Becker A 2011 *Phys. Rev.* A **83** 013414
[11] Liu C and Nisoli M 2012 *Phys. Rev.* A **85** 053423
[12] Palacios A, González-Castrillo A and Martín F 2014 *J. Phys. B: At. Mol. Opt. Phys.* **47** 124013
[13] Dahlström J M, L'Huillier A and Maquet A 2012 *J. Phys. B: At. Mol. Opt. Phys.* **45** 183001
[14] Mauritsson J, Johnsson P, Gustafsson E, L'Huillier A, Schafer K J and Gaarde M B 2006 *Phys. Rev. Lett.* **97** 013001
[15] Aseyev S A, Ni Y, Frasinski L J, Muller H G and Vrakking M J J 2003 *Phys. Rev. Lett.* **91** 223902
[16] Guyétand O *et al* 2005 *J. Phys. B: At. Mol. Opt. Phys.* **38** L357
[17] Guyétand O *et al* 2008 *J. Phys. B: At. Mol. Opt. Phys.* **41** 051002
[18] Picard Y J *et al* 2014 *Phys. Rev.* A **89** 031401
[19] Weber S J *et al* 2015 *Rev. Sci. Instrum.* **86** 033108
[20] Galán A J, Argenti L and Martín F 2013 *New J. Phys.* **15** 113009
[21] Maquet A and Taïeb R 2007 *J. Mod. Opt.* **54** 1847–57
[22] Meyer M *et al* 2008 *Phys. Rev. Lett.* **101** 193002
[23] Yudin G L, Patchkovskii S, Corkum P B and Bandrauk A D 2007 *J. Phys. B: At. Mol. Opt. Phys.* **40** F93
[24] Yudin G L, Chelkowski S and Bandrauk A D 2006 *J. Phys. B: At. Mol. Opt. Phys.* **39** L17
[25] Boll D I R and Fojón O A 2014 *Phys. Rev.* A **90** 053414
[26] Boll D and Fojón O A 2016 *J. Phys. B: At. Mol. Opt. Phys.* **49** 185601
[27] Kazansky A K and Kabachnik N M 2007 *J. Phys. B: At. Mol. Opt. Phys.* **40** 2163
[28] Neidel C *et al* 2013 *Phys. Rev. Lett.* **111** 033001
[29] Gradshteyn I S and Ryzhik I M 2007 *Table of Integrals, Series, and Products* 7th edn (Amsterdam: Elsevier)
[30] Schmidt M W *et al* 1993 *J. Comput. Chem.* **14** 1347–63
[31] Ema I, García de la Vega J M, Ramírez G, López R, Fernández R J, Meissner H and Paldus J 2003 *J. Comput. Chem.* **24** 859–68
[32] Stewart R F 1970 *J. Chem. Phys.* **52** 431–8
[33] Yudin G L, Patchkovskii S and Bandrauk A D 2008 *J. Phys. B: At. Mol. Opt. Phys.* **41** 045602
[34] Yudin G L, Chelkowski S, Itatani J, Bandrauk A D and Corkum P B 2005 *Phys. Rev.* A **72** 051401
[35] Chelkowski S, Yudin G L and Bandrauk A D 2006 *J. Phys. B: At. Mol. Opt. Phys.* **39** S409
[36] Bandrauk A D, Chelkowski S, Corkum P B, Manz J and Yudin G L 2009 *J. Phys. B: At. Mol. Opt. Phys.* **42** 134001
[37] Mauritsson J, Gaarde M B and Schafer K J 2005 *Phys. Rev.* A **72** 013401
[38] Walter M and Briggs J 1999 *J. Phys. B: At. Mol. Opt. Phys.* **32** 2487
[39] Ciappina M F, Fojón O A and Rivarola R D 2014 *J. Phys. B: At. Mol. Opt. Phys.* **47** 042001